Acta Pharmaceutica Sinica B 2015;5(6):569–576

HOSTED BY

Chinese Pharmaceutical Association
Institute of Materia Medica, Chinese Academy of Medical Sciences

Acta Pharmaceutica Sinica B

www.elsevier.com/locate/apsb
www.sciencedirect.com

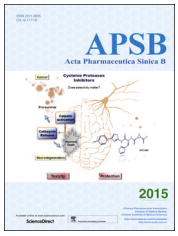

ORIGINAL ARTICLE

Pharmacokinetic and pharmacodynamic study of triptolide-loaded liposome hydrogel patch under microneedles on rats with collagen-induced arthritis

Gui Chen[a,c], Baohua Hao[a,*], Dahong Ju[b], Meijie Liu[b], Hongyan Zhao[b], Zhongping Du[b], Jizi Xia[c]

[a]*School of Life and Science, Northwest University, Xi'an 710069, China*
[b]*Institute of Theory, China Academy of Traditional Chinese Medicine, Beijing 100700, China*
[c]*Qiannan Institute for Food and Drug Control, Duyun 558000, China*

Received 10 June 2015; received in revised form 27 July 2015; accepted 16 September 2015

KEY WORDS

Pharmacokinetics;
Pharmacodynamics;
Triptolide;
Micro-electro-mechanical system;
Microneedles;
Collagen-induced arthritis

Abstract Triptolide (TP), a major active component of *Tripterygium wilfordii* Hook.F. (TWHF), is used to treat rheumatoid arthritis (RA). However, it has a narrow therapeutic window due to its serious toxicities. To increase the therapeutic index, a new triptolide-loaded transdermal delivery system, named triptolide-loaded liposome hydrogel patch (TP-LHP), has been developed. In this paper, we used a micro-needle array to deliver TP-LHP to promote transdermal absorption and evaluated this treatment on the pharmacokinetics and pharmacodynamics of TP-LHP in a rat model of collagen-induced arthritis (CIA). The pharmacokinetic results showed that transdermal delivery of microneedle TP-LHP yielded plasma drug levels which fit a one-compartment open model. The relationship equation between plasma concentration and time was $C=303.59\times(e^{-0.064t}-e^{-0.287t})$. The results of pharmacodynamic study demonstrated that TP-LHP treatment mitigated the degree of joint swelling and suppressed the expressions of fetal liver kinase-1, fetal liver tyrosine kinase-4 and hypoxia-inducible factor-1α in synovium. Other indicators were also reduced by TP-LHP, including hyperfunction of immune, interleukin-1β and interleukin-6 levels in serum. The therapeutic mechanism of TP-LHP might be regulation of the balance between Th1 and Th2, as well as inhibition of the expression and biological effects of vascular endothelial growth factor.

© 2015 Chinese Pharmaceutical Association and Institute of Materia Medica, Chinese Academy of Medical Sciences. Production and hosting by Elsevier B.V. This is an open access article under the CC BY-NC-ND license (http://creativecommons.org/licenses/by-nc-nd/4.0/).

*Corresponding author. Tel.: +86 29 81970519.
E-mail address: haobaohua211@126.com (Baohua Hao).

Peer review under responsibility of Institute of Materia Medica, Chinese Academy of Medical Sciences and Chinese Pharmaceutical Association.

http://dx.doi.org/10.1016/j.apsb.2015.09.006

2211-3835 © 2015 Chinese Pharmaceutical Association and Institute of Materia Medica, Chinese Academy of Medical Sciences. Production and hosting by Elsevier B.V. This is an open access article under the CC BY-NC-ND license (http://creativecommons.org/licenses/by-nc-nd/4.0/).

1. Introduction

Triptolide (Fig. 1A), a major active diterpenoid triepoxide isolated from the traditional Chinese medicine *Tripterygium wilfordii* Hook.F. (TWHF), has multiple pharmacological activities including anti-inflammatory, immune-suppressive, anti-tumor and anti-fertility activity[1–3]. It has been reported to be effective in the treatment of inflammatory and autoimmune diseases, especially rheumatoid arthritis (RA)[4]. However, the clinical uses of triptolide are largely limited because of its severe toxicities, such as gastrointestinal, liver, cardiac, hematopoietic system and urogenital toxicity[5]. In China, the incidence of adverse reactions is over 60%, especially in the gastrointestinal tract, *e.g.*, nausea, vomiting, cramping, diarrhea, and duodenal ulcer[6]. Transdermal delivery systems can often bypass hepatic first pass metabolism and reduce the incidence or severity of gastrointestinal reactions[7]. Therefore, a transdermal delivery system could have significant advantages in the clinical use of triptolide.

The nature of human skin poses significant impediments for transdermal drug delivery. Human skin is mainly composed of three parts: cuticle, epidermis and dermis layer. Cuticle, the outermost layer of skin, is the biggest barrier to percutaneous absorption. Although some chemical penetration enhancers have been used for transdermal drug delivery, but macromolecular drugs (proteins, peptides, polysaccharides) do not easily penetrate the skin[8]. Microneedles can break the barrier of skin, and flat tips are better than sharp tips for enhancing skin permeability[9].

Collagen-induced arthritis (CIA) in the rat is a widely studied animal model of inflammatory polyarthritis with similarities to RA, and primarily mediated by an autoimmune response[10]. Because of many similarities between CIA and RA, the CIA model is the most widely used for the study of RA[11].

Interleukin-1β (IL-1β) and interleukin-6 (IL-6) are involved in the regulation of the immune response, hematopoiesis, and inflammatory[12]. Two high-affinity vascular endothelial growth factor (VEGF) receptors, fetal liver tyrosine kinase-1(Flt-1)/VEGFR-1 and fetal liver kinase-1(Flk-1)/VEGFR-2, play important role during neovascularization[13]. Flt-4/VEGFR-3 has a critical function in the remodeling of the primary capillary vasculature of midgestation embryos. Later during development, Flt-4 regulates the growth and maintenance of the lymphatic vessels[14]. Hypoxia-inducible factor-1α (HIF-1α) is a master regulator of tissue adaptive responses to hypoxia, and has a direct regulatory effect on both survival and function in inflammatory microenvironments[15].

In this paper, using andrographolide (Fig. 1B) as an internal standard (IS), we established a new method for the quantitation of triptolide in CIA rat plasma. The aim of this study was to develop a novel formulation of triptolide and investigate the pharmacokinetics and pharmacodynamics of microneedle-applied TP-LHP on rats with CIA. The findings will help to improve the development of topical formulations of TP-LHP and to optimize the therapeutic use of this drug.

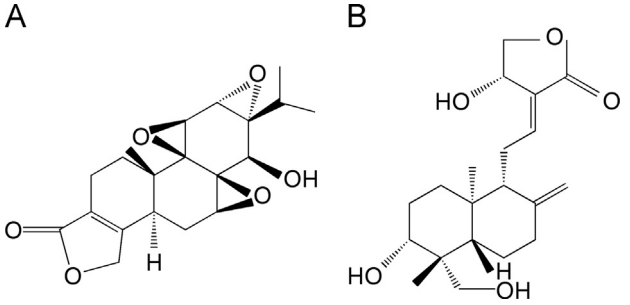

Figure 1 Structures of (A) triptolide and (B) andrographolide (IS).

2. Experimental

2.1. Animals

Sprague-Dawley male rats (8–9 weeks) weighing 180–200 g were purchased from the Laboratory Animal Center of the Fourth Military Medical University (Shanxi, China). The animal experiments were approved by the Institutional Animal Ethics Committee.

2.2. Chemicals and reagents

Triptolide and andrographolide were purchased from the National Institute for the Control of Pharmaceutical and Biological Products (Beijing, China). Bovine type II collagen and incomplete Freund's adjuvant were bought from Chondrex, inc. (Redmond, WA, USA). Interleukin-1β and interleukin-6 ELISA test kits were obtained from eBioscience® Company (Vienna, Austria). Flk-1, Flt-4 and HIF-1α antibody were purchased from Thermo Scientific (Fremont, CA, USA). HPLC grade methanol was obtained from Sigma-Aldrich (Shanghai) Trading Co., Ltd. (Shanghai, China). Deionized water was purified with a Milli-Q system (Millipore, Milford, MA, USA). Other chemicals were of analytical grade.

2.3. Preparation of CIA model and evaluation of arthritis

The collagen II (CII) was mixed with an equal volume of incomplete Freund's adjuvant and emulsified. The emulsion was checked by the non-dispersability of a drop of the emulsion in water. Rats were injected subcutaneously at the root of the tail with 0.2 mL of the CII emulsion. A booster immunization with 0.1 mL of the CII emulsion was performed in the same manner after a week. Starting from the second week after immunization, the degree of arthritis was measured by Plethysmometer (paw volume) every week (Fig. 2). The formula was $P=(V-V_0)/V_0\times 100\%$, where P represents degree of joint swelling, V represents the volume after inflammation and V_0 represents the volume before inflammation.

2.4. Preparation of triptolide-loaded liposome hydrogel patch

Liposomes were formed by the known film dispersion method. Liposome size and encapsulation efficiency were measured to assess this method. The polydispersity index of size distribution was described by nanometer laser particle size and zeta potential analyzer. The encapsulation efficiency was measured by HPLC, and calculated by the formula $P=(W-W_1)/W\times 100\%$, where P represents encapsulation efficiency, W represents the total content of triptolide in liposomes, and W_1 represents the content of free triptolide. Egg lecithin (450.0 mg), cholesterol (90.0 mg), and triptolide (20.0 mg) were dissolved in ethanol (50 mL), and the solution was poured into a 250 mL round-bottomed flask. Then solvent was evaporated to dryness on a rotary evaporator under reduced pressure and lipid film thereby obtained was then dispersed in water (50 mL). The liposome preparation was filtered with a membrane filter (0.22 μm pore size) and used. The average of liposome size was 201.52 ± 18.43 nm with an encapsulation efficiency of $83.62\pm 1.97\%$.

Viscomate NP-700 (5.60 g), glycine aluminum (0.35 g), polyvinylpyrrolidone K-90 (4.20 g), and triptolide liposome (22.4 mL)

were dissolved in glycerin (35.00 g) as phase A. Tartaric acid (0.49 g) was dissolved in distilled water (80 mL) as phase B. Phase B was then added to phase A and mixed by stirring slowly. The liposomes still maintain the original structure after mixed in glycerin with phase B revealed by transmission electron microscopy. The ointment was coated onto woven fabrics. The last step was film mulching after gelation, and TP-LHP was prepared.

2.5. *Instrument and analytical conditions*

The liquid chromatographic system consisted of two LC-20AT pumps, a Shimadzu 10ATvp auto sampler, a CTO-10Avp column oven, a SPD-20A detector and a CBM-10Avp Plus chromatographic station (Shimadzu, Kyoto, Japan). Analyses were performed on a Shim-pack VP-DOS C18 analytical column (250 mm × 4.6 mm i.d., particle size 5 μm, Shimadzu, Kyoto, Japan), which was protected by a ODS guard column (Security Guard, Phenomenex®, USA) at 30 °C. The mobile phase was composed of methanol/water (45:55, *v/v*) at a flow rate of 0.50 mL/min. The detection wavelength was set at 218 nm. Under these conditions, triptolide eluted at approximately 15 min and the internal standard at 25 min (Fig. 3).

2.6. *Preparation of stock solutions and quality control samples*

The standard stock solution (1 mg/mL) of triptolide was obtained in methanol. A series of standard working solutions, consisted of seven

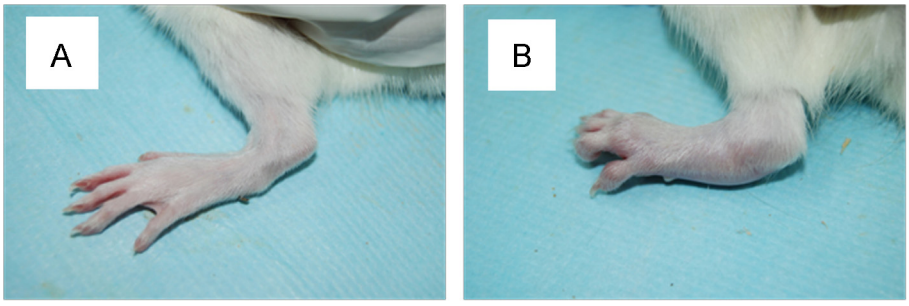

Figure 2 Comparison of rats (A) before and (B) after modeling CIA.

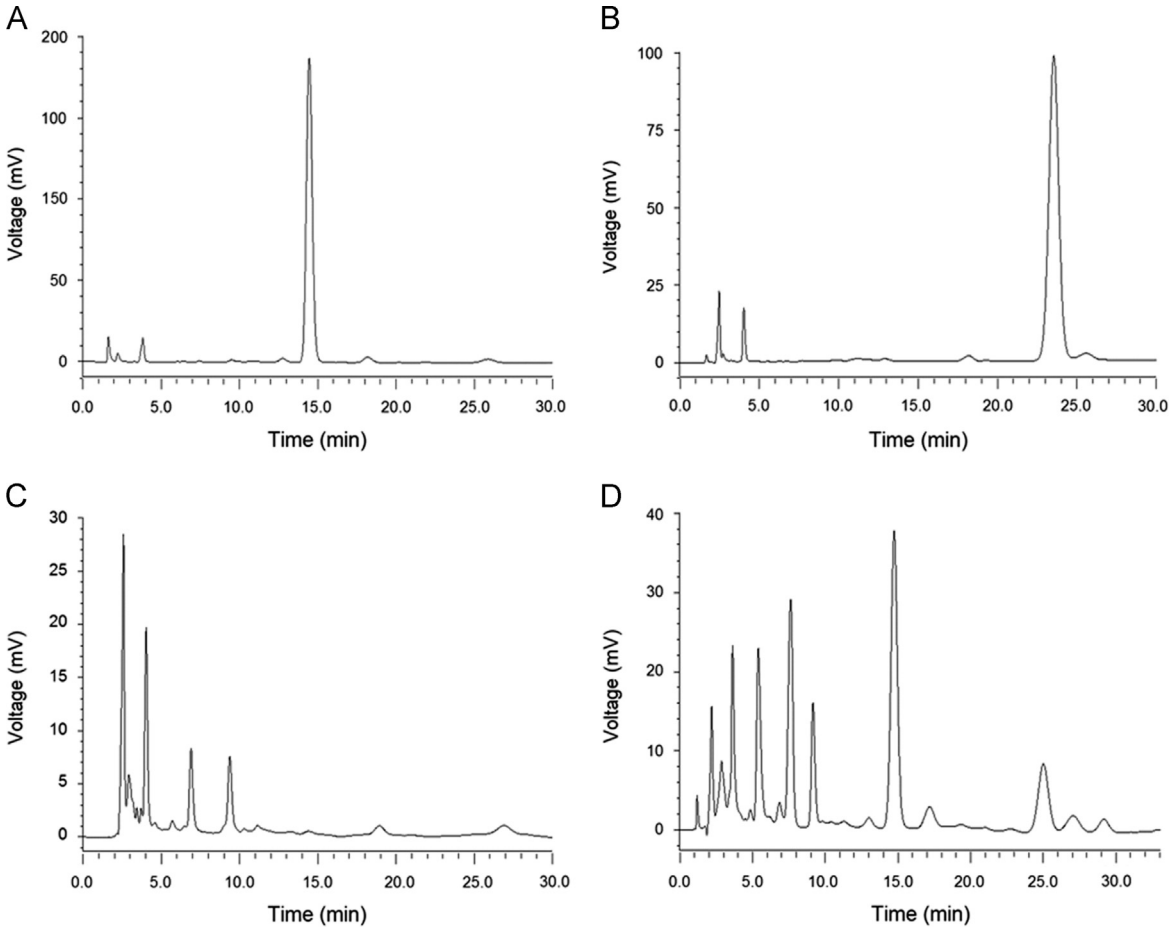

Figure 3 HPLC chromatograms of (A) triptolide, (B) andrographolide, (C) plasma sample and (D) plasma spiked with triptolide and andrographolide.

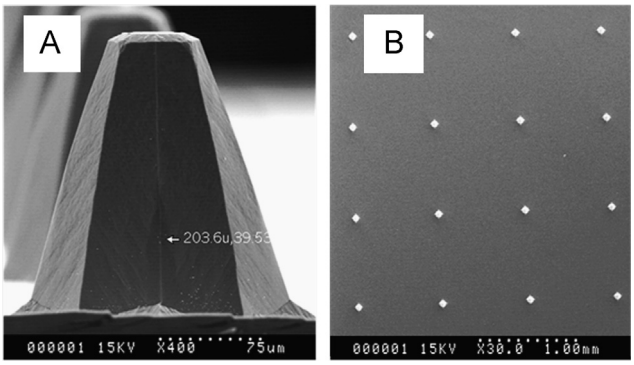

Figure 4 Electron micrographs of microneedles. (A) 200 μm microneedles; (B) 200 μm microneedle array.

Table 1 Precision of intra- and inter-day of HPLC assay for determining triptolide in plasma samples.

Nominal concentration (ng/mL)	Precision (RSD, %)	
	Intra-day ($n=5$)	Inter-day ($n=3$)
25	6.8	7.3
100	5.7	6.4
500	4.9	5.3

Table 2 Stability of HPLC assay for determining triptolide in plasma samples.

Nominal concentration (ng/mL)	RSD (%, $n=5$)		
	Freeze–thaw	At 4 °C, 12 h	At −20 °C, 3 weeks
25	6.2	6.9	9.2
100	4.7	7.5	8.3
500	5.6	5.8	6.5

concentration levels (1.0, 2.5, 5, 10, 25, 50 and 100 μg/mL), were prepared by further dilution of the standard stock solutions with methanol. IS working solution (500 ng/mL) was prepared by diluting IS stock solution with methanol. Working solutions were diluted with drug-free plasma, and obtained a calibration standard range of 10–1000 ng/mL. Samples used in quality control (25, 100 and 500 ng/mL of triptolide in rat plasma) were prepared in the same way.

2.7. *Preparation of samples*

The plasma (0.5 mL) was spiked with 50 μL of IS working solution, after which it was vortex-mixed for 30 s and extracted with ethyl acetate (1 mL) by vortex mixing for 2 min. This tube was then centrifuged at 4000 rpm for 5 min. The upper organic phase was transferred into a new tube and dried under nitrogen. Subsequently, the residues were reconstituted in 150 μL methanol and centrifuged at 14,000 rpm for 10 min after vortex mixing, and 10 μL supernatant was injected into the column for analysis.

Table 3 Extraction recovery of HPLC assay for determining triptolide in plasma samples.

Nominal concentration (ng/mL)	Extraction recovery[a] (%)
25	79.14 ± 8.15
100	83.04 ± 3.39
500	85.37 ± 4.26

[a]Extraction recovery (%) = Concentration found/Concentration added × 100. Data are expressed as mean ± SD, $n=5$.

2.8. *Pharmacokinetic study*

Twelve CIA rats were divided into two groups randomly: group A (i.g. administration) and group B (TP-LHP under microneedles). After an overnight fast (withdrawing food but not water), group A was given a single dose (0.40 mg/kg) of triptolide formulated in 20% propylene glycol aqueous solution (*v*/*v*). Group B was pierced by 200 μm microneedle array (5 N force, 1 min) which was linked to a thrust meter and then pasted TP-LHP with 1.6 mg/kg triptolide. Fig. 4A and B showed the electron micrographs of 200 μm microneedles and 200 μm microneedle arrays. About 0.5 mL of blood samples were collected from the retro-orbital venous plexus with heparinized capillary tubes before (0 h) and at 0.083, 0.25, 0.5, 1, 1.5, 2, 4, 6, 8, 10 and 12 h after dosing in group A, while we collected the blood samples before (0 h) and 0.5, 1, 2, 4, 6, 8, 10, 12, 16, 20, 24 and 28 h after dosing in group B. Plasma was separated by centrifugation at 8000 rpm for 10 min.

2.9. *Pharmacodynamic study*

Nine normal rats were randomly selected as normal group, and 36 rats with CIA were divided into four groups, which are CIA group, TP-LHP low dose group, TP-LHP middle dose group, and TP-LHP high dose group. Two weeks after successfully modeling CIA, normal and model groups were given 200 μm, micro-electro-mechanical system (MEMS) micro-needle array to deal with bilateral hind (at the force of 5 N for 1 min), and then paste the blank TP-LHP. Three TP-LHP treated groups were given the same treatment with 200 μm micro-needle array. The doses of triptolide were 10 mg/kg, 20 mg/kg, and 40 mg/kg, respectively. Medication was administered continuously for four weeks.

2.10. *ELISA assay*

Blood samples were taken *via* the groin artery of rats under ether anesthesia and the serum was obtained by centrifugation at 2500 rpm for 20 min. IL-1β and IL-6 levels in serum were determined by ELISA test kits.

2.11. *Immunohistochemistry assay*

The expressions of Flk-1, FLT-4 and HIF-1α in synovium were detected by immunohistochemistry assay. Positive expression averages of 9 samples (3 scoops in each sample) in each group were determined by Leica-Qwin Image Analysis (Leica Microsystems, Germany). The percentage of positive expression in the whole screened area was calculated.

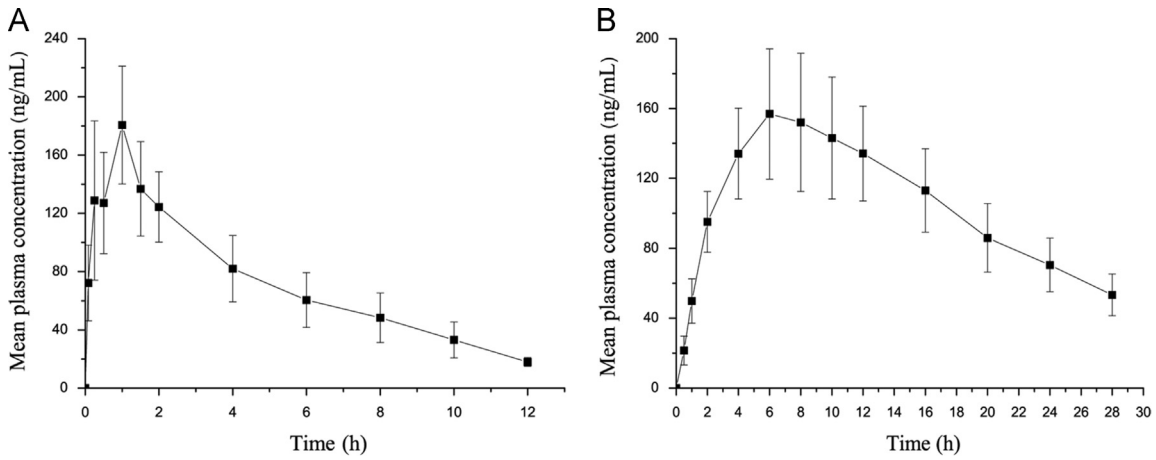

Figure 5 Mean plasma concentration–time profile of triptolide ($n=6$). (A) After i.g. administration at a single dose of 0.4 mg/kg triptolide solution; (B) After transdermal delivery of TP-LHP with 1.6 mg/kg of triptolide under microneedles.

Table 4 Pharmacokinetic parameters of triptolide by i.g. administration and transdermal delivery under microneedles.

Parameter	Unit	Administration method	
		i.g.	Transdermal
$t_{1/2}$ (K)	h	0.595 ± 0.321	10.831 ± 3.414
$t_{1/2}$ (K_a)	h	0.497 ± 0.115	2.410 ± 0.896
$t_{1/2\beta}$	h	2.584 ± 0.766	20.853 ± 5.729
T_{max}	h	0.982 ± 0.282	6.592 ± 1.591
C_{max}	ng/mL	182.46 ± 47.691	153.32 ± 26.463
$AUC_{0\to\infty}$	ng.h/mL	773.63 ± 68.34	4038.45 ± 527.74

Data are expressed as mean ± SD, $n=5$.

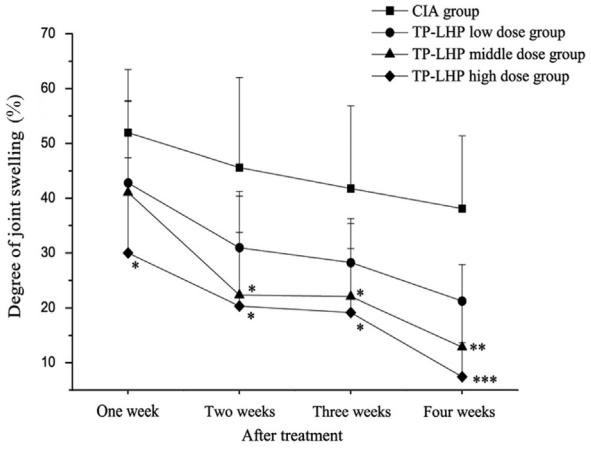

Figure 6 Changes on degree of joint swelling in CIA and TP-LHP treated groups. $^{*}P<0.01$, $^{**}P<0.01$, $^{***}P<0.001$ *vs.* CIA group, $n=9$.

2.12. Statistical analysis

All data were expressed in mean ± standard deviation (SD) and analyzed *via* SPSS 18.0 software. Statistical significance was determined using repeated-measures ANOVA, one-way ANOVA and LSD-t test, with P-values <0.05 regarded as statistically significant.

3. Results

3.1. Method validation

3.1.1. Linearity

Calibration curves are plotted as the peak area ratio (triptolide/IS) *versus* triptolide concentrations. The calibration curves show good linearity ($R^2=0.9991$) over the concentration range of 10–1000 ng/mL. The best fit linear regression equation is $y=0.1069\ x+0.0057$, where x represents triptolide concentration in ng/mL and y represents triptolide area/IS area.

3.1.2. Precision

Table 1 displays the precision of the HPLC method for determining of triptolide in plasma samples. The intra-day precision (RSD) ranged 4.9%–6.8% and the inter-day precision ranged 5.3%–7.3%. Thus, the method has a satisfactory precision and reproducibility.

3.1.3. Stability

Table 2 shows the stability of triptolide under following conditions: (1) three freeze–thaw cycles, (2) 4 °C for 12 h, (3) −20 °C for 3 weeks. As a result, triptolide showed good stability at the three conditions.

3.1.4. Recovery

The extraction recovery of triptolide was above 80% on average (Table 3), and the dependence on concentration was negligible. The recovery of IS was 75.26% at the concentration used in the assay (500 ng/mL).

3.2. Pharmacokinetic study

The HPLC method was successfully used for the pharmacokinetic study following i.g. administration at a single dose of 0.4 mg/kg triptolide solution and transdermal delivery of TP-LHP under micro-needle. The mean plasma concentration–time profiles for triptolide are shown in Fig. 5. The pharmacokinetic parameters of triptolide were calculated by Drug and Statistics (DAS) software. The main pharmacokinetic parameters are shown in Table 4. Transdermal delivery of micro-needle TP-LHP yielded plasma

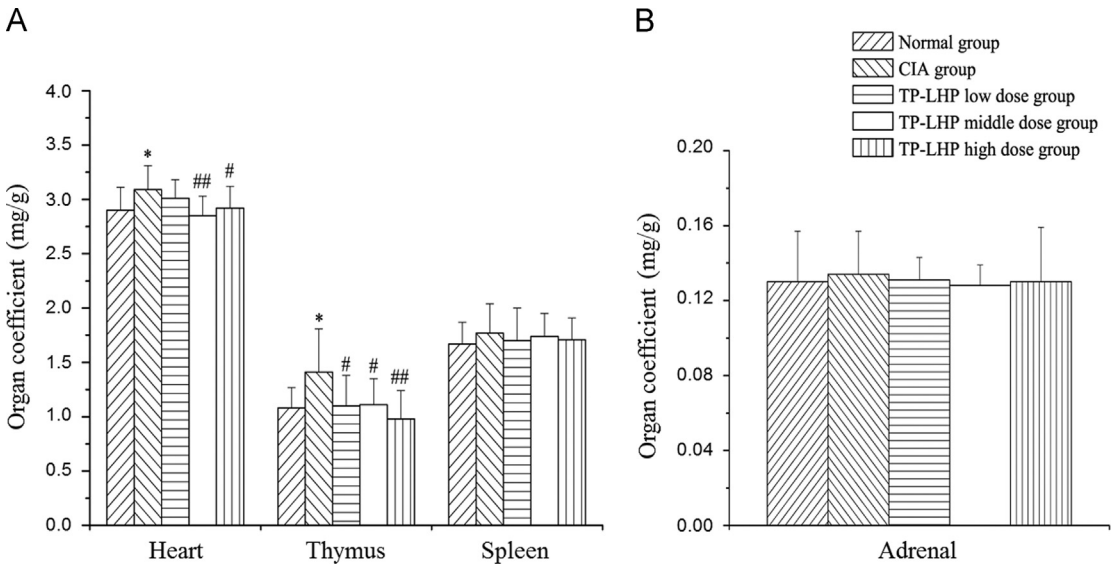

Figure 7 The organ coefficients of (A) heart, thymus, and spleen and (B) adrenal. $^{*}P<0.05$ *vs*. control group; $^{\#}P<0.05$, $^{\#\#}P<0.01$ *vs*. CIA group, $n=9$. There was no significant difference in the organ coefficients of spleen and adrenal in each group.

drug profiles which fit the one-compartment open model. The relationship equation between plasma concentration and time was $C=303.59\times(e^{-0.064t}-e^{-0.287t})$.

3.3. *Degree of joint swelling*

Fig. 6 shows the changes in joint swelling in the CIA and TP-LHP groups. The degree of joint swelling in TP-LHP high dose group was significantly decreased from the first week after treatment (*vs*. CIA group, $^{*}P<0.05$). Both middle and high dose of TP-LHP obviously decreased the degree of joint swelling from the second week to the third week ($^{*}P<0.05$), and the difference was more pronounced at the fourth week ($^{**}P<0.01$, $^{***}P<0.001$).

3.4. *Organ coefficient*

Fig. 7 shows the organ coefficients of heart, thymus, adrenal and spleen. There was no significant difference in the organ coefficients of adrenal and spleen in each group. Higher organ coefficient of heart was found in the rats of CIA group ($^{*}P<0.05$ *vs*. normal group), while TP-LHP at all dose levels could reverse this change ($^{\#}P<0.05$, $^{\#\#}P<0.01$ *vs*. CIA group). However, TP-LHP at middle dose had more significant difference. Attention should be paid to this, as the organ coefficient of heart could increase with the dose.

3.5. *IL-1β and IL-6 level in serum*

Fig. 8 shows the IL-1β and IL-6 level in serum. Higher levels of IL-1β were found in serum of CIA group and low-dose TP-LHP treated group ($^{*}P<0.05$ *vs*. normal group), while lower levels of IL-1β were observed in serum of middle-dose and high-dose TP-LHP treated groups ($^{\#}P<0.05$, $^{\#\#\#}P<0.001$ *vs*. CIA group). The rats in CIA group showed higher serum level of IL-6 ($^{***}P<0.001$ *vs*. normal group). TP-LHP at all dose levels could reverse the change of IL-6 ($^{\#\#}P<0.01$, $^{\#\#\#}P<0.001$ *vs*. CIA group).

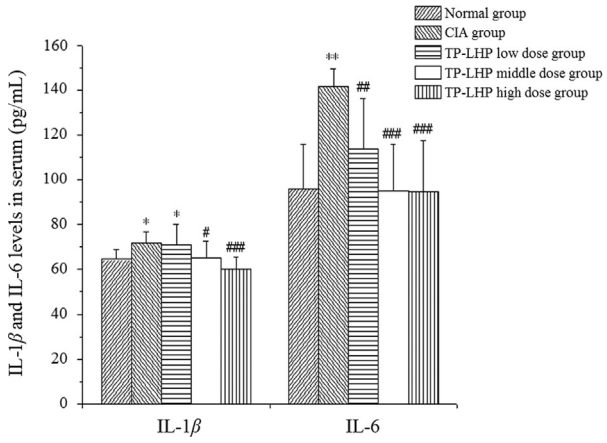

Figure 8 Changes on IL-1β and IL-6 level in serum. $^{*}P<0.05$, $^{**}P<0.001$ *vs*. normal group; $^{\#}P<0.05$, $^{\#\#}P<0.01$, $^{\#\#\#}P<0.01$ *vs* CIA group; $n=9$.

3.6. *Changes on Flk-1, Flt-4 and HIF-1α expression in synovium*

Fig. 9 A–F shows the expressions of Flk-1, Flt-4, and HIF-1α in synovium, whereas Fig. 9G shows the percentage of the positive expression in synovium. Higher expression levels of Flk-1 were found in CIA, TP-LHP low dose and middle dose group ($P<0.001$, *vs*. normal group) and TP-LHP at high dose level could reverse this change ($P<0.001$, *vs*. CIA group). Although the expression of Flk-1 in TP-LHP low-dose group also decreased, the difference was not significant.

Higher expression levels of Flt-4 were found in the CIA group ($P<0.001$, *vs*. normal group), while TP-LHP at middle and high dose levels could reverse this change ($P<0.001$, *vs*. CIA group). Although the expression of Flt-4 in TP-LHP low-dose group also decreased, the difference was not significant.

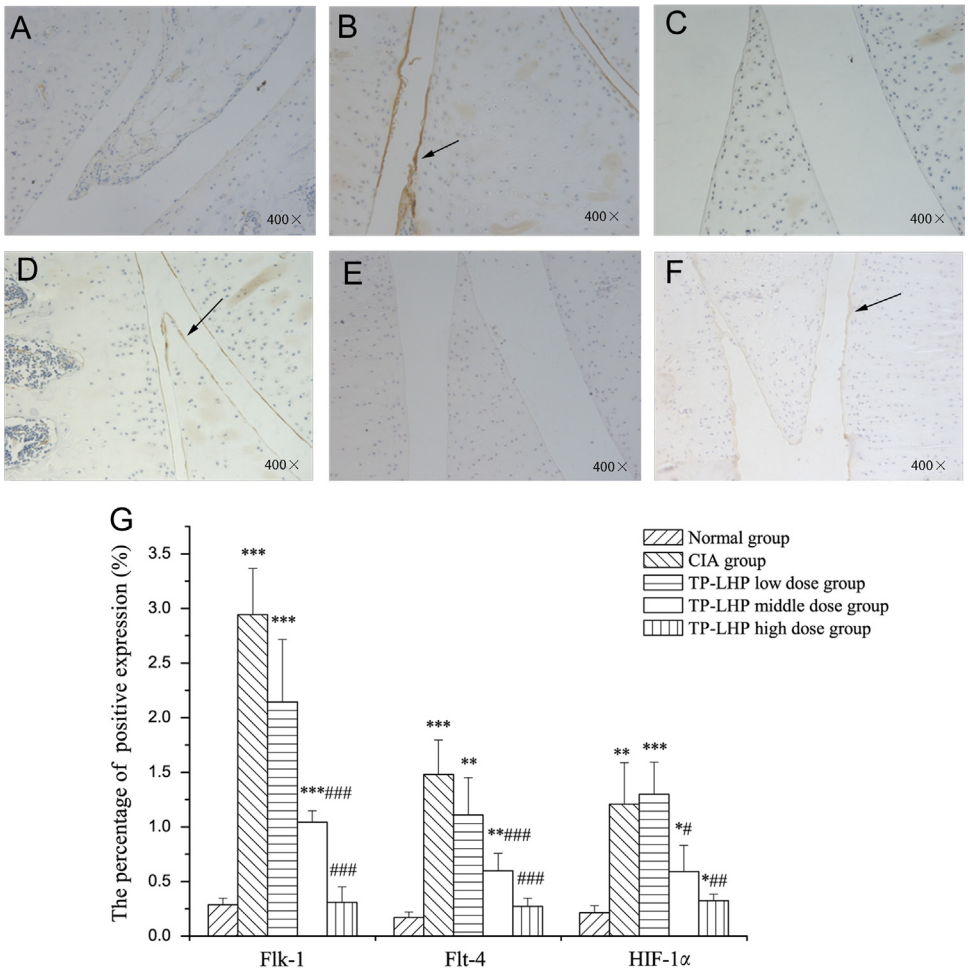

Figure 9 The expressions of Flk-1, Flt-4, and HIF-1α in synovium. (A) Flk-1 in normal group; (B) Flk-1 in CIA group; (C) Flt-4 in normal group; (D) Flt-4 in CIA group; (E) HIF-1α in normal group; (F) HIF-1α in CIA group. The brown–yellow stains were defined as the positive expressions. (G) The percentage of the positive expression of Flk-1, Flt-4 and HIF-1α in synovium. $^{*}P<0.05$, $^{**}P<0.01$, $^{***}P<0.001$ *vs*. normal group; $^{\#}P<0.05$, $^{\#\#}P<0.01$, $^{\#\#\#}P<0.001$ *vs*. CIA group; $n=9$.

Figure 10 Histological section of rat skin pierced by 200 μm microneedles.

Higher expression levels of HIF-1α were found in CIA and TP-LHP low dose group ($^{**}P<0.01$, $^{***}P<0.001$, *vs*. normal group), while TP-LHP at middle and high dose levels could reverse this change ($^{\#}P<0.05$, $^{\#\#}P<0.01$, *vs*. CIA group).

4. Discussion

The present findings confirmed that microneedles can pierce the skin and form conduits (Fig. 10) which enhance transdermal drug delivery.

Compared with i.g. administration, TP-LHP had a slower time-to-peak and longer stability of plasma concentration. There was a significant increase in the $AUC_{0\rightarrow\infty}$, which indicated that TP-LHP improved the bioavailability of triptolide.

The degree of joint swelling was mitigated by TP-LHP at all dose levels. There was a significant change after one week's treatment in TP-LHP high dose group. Drug administration over 2–3 weeks achieved a smooth period in which the degree of joint swelling had no obvious changes. After four weeks' treatment, joint swelling was further mitigated. The mechanism for these effects may be that triptolide inhibited formation and release of inflammatory mediators.

There were no significant differences between spleen coefficient and adrenal coefficient in each group, while the thymus coefficients in CIA group and TP-LHP low-dose group were significantly higher than normal group. The CIA model induced by collagen II, an immune hyperthyroidism model, produced arthritis symptoms which were significantly mitigated by high doses of TP-LHP.

The heart coefficient in CIA group was significantly higher than normal group. The reason might be that RA increased cardiac load. TP-LHP at low dose had no significant effect on heart coefficient of CIA model, while TP-LHP at middle and high doses produced significant reductions. These results showed that TP-LHP at certain doses can improve RA and reduce heart damage. However, the heart coefficient increased with the increased doses, suggesting that overdose of TP-LHP might cause heart damage.

Significant effects on IL-1β levels were found in the middle and high-dose TP-LHP groups, and IL-6 levels were remarkably reduced by TP-LHP at all doses. This indicates that therapeutic action of TP-LHP might relate to the regulation of Th1/Th2 balance.

The results of immunohistochemistry assays indicated that TP-LHP produced dose-related inhibition of the expression of Flk-1, Flt-4 and HIF-1α. TP inhibited the expression of Flk-1 and Flt-4 which are VEGF receptors. Thus TP-LHP inhibited the biological effects of VEGF mediated by Flk-1 and Flt-4. Inhibiting the expression of HIF-1α, TP declined the expression of VEGF induced by HIF-1α. Therefore, suppressing the expression and biological effects of VEGF is an important mechanism for the therapeutic effects of TP-LHP.

5. Conclusions

Microneedle technology can be used in topical formulations for enhancement of drug delivery. When triptolide was prepared as TP-LHP, the hepatic first-pass metabolism and digestive toxicity were eliminated. TP-LHP provided stable, long-term release of triptolide, and had significant efficacy in the CIA model. The combination of TP-LHP and microneedle technology could provide a safe and efficient administration method of triptolide for treating RA.

Acknowledgment

This study was supported by National Science and Technology Major Project on Significant Creation of New Drugs of China (2009ZX09502-019).

References

1. Panichakul T, Intachote P, Wongkajorsilp A, Sripa B, Sirisinha S. Triptolide sensitizes resistant cholangiocarcinoma cells to TRAIL-induced apoptosis. *Anticancer Res* 2006;**26**:259–65.
2. Brinker AM, Ma J, Lipsky PE, Raskin I. Medicinal chemistry and pharmacology of genus *Tripterygium* (Celastraceae). *Phytochemistry* 2007;**68**:732–66.
3. Liu QY. Triptolide and its expanding multiple pharmacological functions. *Int Immunopharmacol* 2011;**11**:377–83.
4. Zhou GS, Hu Z, Fang HT, Zhang FX, Pan XF, Chen XQ, et al. Biologic activity of triptolide in *t*(8;21) acute myeloid leukemia cells. *Leukemia Res* 2011;**35**:214–8.
5. Liu L, Jiang ZZ, Liu J, Huang X, Wang T, Liu J, et al. Sex differences in subacute toxicity and hepatic microsomal metabolism of triptolide in rats. *Toxicology* 2010;**271**:57–63.
6. Wang B, Jiang ZZ, Zhang LY. Advances in studies on toxicity and attenuation of triptolide. *Drug Eval Res* 2012;**35**:211–5.
7. Sarkar V, Yadav KC. Formulation and evaluation of prolonged release transdermal drug delivery system of atenolol for the treatment of hypertension. *Pharmtutor* 2014;**2**:134–40.
8. Pathan Setty IB. CM. Chemical penetration enhancers for transdermal drug delivery systems. *Int J Pharm* 2009;**8**:172–9.
9. Li WZ, Huo MR, Zhou JP, Zhou YQ, Hao BH, Liu T, et al. Super-short solid silicon microneedles for transdermal drug delivery applications. *Int J Pharm* 2010;**389**:122–9.
10. Anthony DD, Haqqi TM. Collagen-induced arthritis in mice: an animal model to study the pathogenesis of rheumatoid arthritis. *Cli Exp Rheumatol* 1999;**17**:240–4.
11. Xiao C, Zhao LH, Liu ZL, Lu C, Zhao N, Yang DJ, et al. The effect of triptolide on CD4+ and CD8+ cells in the Peyer's patch of DA rats with collagen induced arthritis. *Nat Prod Res* 2009;**23**:1699–706.
12. Akira S, Hirano T, Taga T, Kishimoto T. Biology of multifunctional cytokines: IL 6 and related molecules (IL 1 and TNF). *FASEB J* 1990;**4**:2860–7.
13. Roberts DM, Kearney JB, Johnson JH, Rosenberg MP, Kumar R, Bautch VL. The Vascular Endothelial Growth Factor (VEGF) Receptor Flt-1 (VEGFR-1) Modulates Flk-1 (VEGFR-2) Signaling During Blood Vessel Formation. *Am J Pathol* 2004;**164**:1531–5.
14. Mäkinen T, Veikkola T, Mustjoki S, Karpanen T, Catimel B, Nice EC, et al. Isolated lymphatic endothelial cells transduce growth, survival and migratory signals *via* the VEGF-C/D receptor VEGFR-3. *EMBO J* 2001;**20**:4762–73.
15. Kubota K, Ito K, Morooka M, Minamimoto R, Miyata Y, Yamashita H, et al. FDG PET for rheumatoid arthritis: basic considerations and whole-body PET/CT. *Ann N Y Acad Sci* 2011;**1228**:29–38.